Effects of Backbone Configuration of Polysilanes on Nanoscale Structures Formed by Single-Particle Nanofabrication Technique

Shu Seki,* Satoshi Tsukuda, Kensaku Maeda, and Seiichi Tagawa*

Institute of Scientific and Industrial Reseach, Osaka University, 8-1 Mihogaoka, Ibaraki, Osaka 567-0047, Japan

Hiromi Shibata

Department of Nuclear Engineering, Faculty of Engineering, Kyoto University, Yoshida Honmachi, Sakyo-ku, Kyoto 606-8501, Japan

Masaki Sugimoto

Japan Atomic Energy Research Institute, Takasaki Radiation Chemistry Research Establishment, 1233 Watanuki-machi, Takasaki, Gumma 370-1292, Japan

Koichi Jimbo, Isao Hashitomi, and Akira Kohyama

Institute of Advanced Energy, Kyoto University, Gokasho, Uji, Kyoto 611-0011, Japan

Received August 17, 2005

ABSTRACT: Ion-beam irradiation of poly(methylphenylsilane) (PMPS) is shown to cause cross-linking reactions, leading to the formation of a polymer gel containing cylindrical nanostructures of regular length and thickness. The spatial distribution of cross-links of polymer molecules is found to be governed by the deposited energy density in an ion track. The radial variation in dose along each ion track results in the formation of cylindrical structures with a radius of 1−12 nm. These cylindrical structures are well visualized by atomic force microscopy as wormlike structures (nanowires). The total volume of the cross-linked polymer gel can be represented by this cylindrical radially varying scheme of cross-link distribution well. As the cross-linking reaction efficiency estimated by conventional statistical theories of polymer gelation overestimate the dependence of the efficiency on the chain length of the polymers, a new formalism is derived considering the dependence of the nanowire size on the chain length, the linear energy transfer of the ion beam, the radial dose distribution in ion tracks, and the global chain configuration of polymers. The resultant model provides a better representation of ion-beam-induced gelation of polymers. The present results also demonstrate the potential utility of this technique for single-particle fabrication of nanostructures with subnanometer spatial resolution.

Introduction

The use of high-energy charged particles has extended to many fields in recent years. In medicine, nonhomogeneous energy deposition along an ion trajectory (ion track) plays a crucial role in cancer radiotherapy,[1] allowing for high spatial selectivity in the distribution of the radiation dose. The direct observation and application of ion tracks in media have also attracted interest in materials science, where it is known as nuclear track fabrication.[2−4] Since the discovery that high-energy particle leave latent tracks in inorganic and organic polymer materials, the technique has also been applied to the production of micro- and nanosized pores in materials through chemical etching of the tracks.[5−7] The clear correlation between the etched pore and the characteristics of the incident charged particle has been utilized for measurement of the velocity and mass of the incident particles, and such organic film detectors are widely used in dosimetry[8] and, in particular, for galactic cosmic rays in space.[9]

The radiation sensitivity of polymers, such as G values (number of reactions per 100 eV of absorbed dose), have been studied extensively for many polymers and types of radiation. The cross-linking of polymers under radiation was formulated by Charlesby on the basis of the statistical mechanics of polymer molecules, giving the G values for cross-linking ($G(x)$) and chain scission ($G(s)$).[10] Cherlesby's theory has been extended by many groups to explain reactions in real polymer systems,[11−14] as the initial formulation was based on an ideal polymer system involving a random distribution of molecular sizes and cross-links and neglecting effects of the solid-state structure of the target polymer. Ion-beam-induced chemical reactions are an exceptional case in that the spatial distribution of the deposited energy by incident ions is nonhomogeneous.[15,16] The specific properties of ion beams have been characterized by the linear energy transfer (LET), given by the energy deposition of an incident particle per unit length, and the effects of LET on the yield of chemical reactions in a medium, particularly cross-linking reactions in polymeric materials, have been investigated extensively.[17−22]

The ion track radius is also an important parameter in such reactions, reflecting the local spatial distribution of energy deposited by an incident ion and influencing the character of subsequent chemical reactions.[15,16,23−27] Our group recently reported on main-chain scission and cross-linking reactions in a variety of polymer systems and proposed chemical core sizes in ion tracks based

* Corresponding authors. E-mail: seki@sanken.osaka-u.ac.jp (S.S.); tagawa@sanken.osaka-u.ac.jp (S.T.). Telephone: +81-6-6879-8502 (S.S.); +81-6-6879-8500 (S.T.). Fax: +81-6-6876-3287 (S.S.); +81-6-6876-3287 (S.T.).

10.1021/ma051821x CCC: $30.25 © 2005 American Chemical Society
Published on Web 10/26/2005

on discussion of the nonhomogeneous spatial distribution of reactions.[16,28−30] Intratrack cross-linking reactions are also of interest with respect to the potential for the direct formation of nanostructured materials as apposed to the nuclear track technique, and materials exhibiting these reactions have been successfully visualized in recent years.[28,29] However, despite the extensive experimental and theoretical study undertaken to date, many factors in the relationship between the ion track structure and the chemical core radius remain unclear. This paper proposes a new formulation that determines the chemical core radius in an ion track based on the initial distribution of deposited energy, the efficiency of the chemical reactions, and the molecular structure of the target polymer materials.

Experiments

All reagents and chemicals were purchased from Wako Pure Chemical Industries unless otherwise noted. Poly(methlphenylsilane) (PMPS) was synthesized by reaction of methlphenyldichlorosilane with sodium in refluxing toluene and undecane[31,32] under an atmosphere of predried argon. Chlorosilane was purchased from Shin-Etsu Chemical and doubly distilled prior to use. The molecular weight distribution of PMPS was measured by gel permeation chromatography (VP-10, Shimadzu), using tetrahydrofuran (THF) as an eluent in a chromatograph equipped with four columns (Shodex KF-805L, Showa Denko). The synthesized PMPS had a bimodal molecular weight distribution, with molecular weight controlled by the reaction time and additives (12-crown-4 and diethleneglycol dimethyl ether as sodium activators). All lots of the obtained PMPS were once mixed and dissolved in toluene, and the fractional precipitates with gradual addition of isopropyl alcohol (IPA) were isolated by centrifugal separation. PMPS was thus separated into 22 lots. The molecular weights of PMPS lots 1−5 used in the present study are summarized in Table.1.

The polymer samples were dissolved in toluene and spin-coated on Si wafers to a thickness of 0.2−1.0 μm. The films were then irradiated in a vacuum chamber ($<1 \times 10^{-6}$ h Pa) with 2 MeV He^+, H^+, C^+, and N^+ ion beams generated by a van de Graaff accelerator at the Research Center for Nuclear Science and Technology, University of Tokyo, with 5.1−10.2 MeV Si^{2+}, Si^{5+}, Fe^{2+}, Fe^{3+}, and Fe^{5+} ion beams generated by the Tandem accelerator at the Institute of Advanced Energy, Kyoto University, and with 175−520 MeV Ar, Kr, and Xe ion beams from the cyclotron accelerator at the Japan Atomic Energy Research Institute of the Takasaki Research Laboratory. The irradiated samples were developed in toluene for 2 min. The irradiated part of the film, where a polymer gel had formed, was insoluble in toluene. The thickness of the film remaining after development was measured by using a surface profiler (Dektak 3ST, Ulvac; SE−2300, Kosaka Laboratory). The normalized thickness was defined as the ratio of the thickness after irradiation to that before. Direct observation of the films after development was carried out by atomic force microscopy (AFM, SPI-3800 and SPI-4000, Seiko Instruments). The loss of kinetic energy of ions due to penetration through the polymer films was estimated using the SRIM 2000 calculation code.[32]

Results and Discussions

Ion-Beam-Induced Gelation in Polymers. Ion-beam irradiation of PMPS films was found to cause gelation of the polymers for all ions, all energies, and all molecular weights of PMPS. Figure 1 shows the sensitivity curves of PMPS films for irradiation with a 2 MeV He^+ ion beam. In the figure, the gel fraction corresponds to the normalized thickness, and the sensitivity curve was calibrated by the absorbed dose (D).

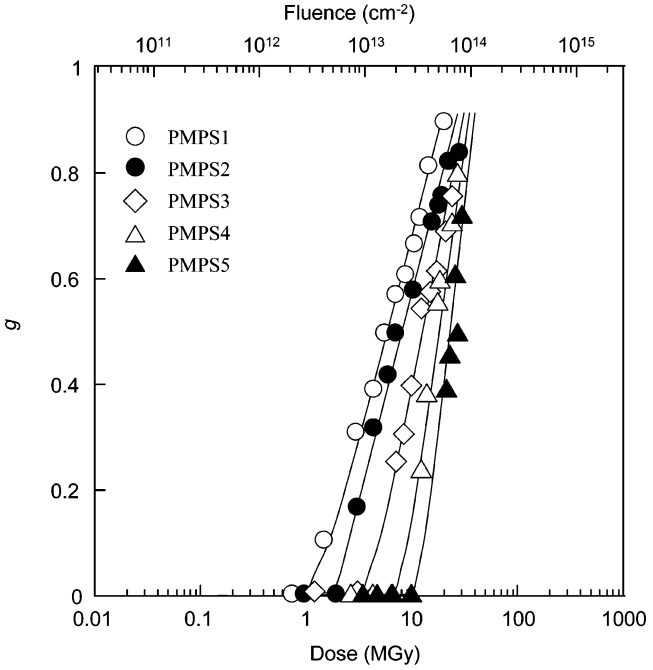

Figure 1. Sensitivity curves (gel evolution curves) for PMPS with various molecular weights under irradiation with a 2 MeV $^4He^+$ beam.

According to the statistical theory of cross-linking and scission of polymers induced by radiation, the G values of cross-linking ($G(x)$) and main-chain scission ($G(s)$) are expressed by the Charlesby−Pinner relationship as follows.[10]

$$s + s^{1/2} = p/q + \frac{m}{q}M_n D \quad (1)$$

$$s = 1 - g \quad (2)$$

$$G(x) = 4.8 \times 10^3 q \quad (3)$$

$$G(s) = 9.6 \times 10^3 p \quad (4)$$

where p is the probability of scission, q is the probability of cross-linking, s is the sol fraction, g is the gel fraction, m is the molecular weight of a unit monomer, and M_n is the number-average molecular weight before irradiation. The cross-linking G values calculated using these equations for irradiation of PMPS with 2 MeV He^+, H^+, C^+, and N^+ ion beams are compared in Table 1. The cross-linking G values for high-molecular-weight PMPS are much lower than those for low-molecular-weight PMPS. Besides chain length, there are no differences in the chemical structures of the polymers, indicating that the efficiency of cross-linking should be identical for all series of polymers to a first approximation. The effects of the molecular weight distribution on the radiation-induced gelation of a real polymer system were considered by Saito[11] and Inokuti,[12] who traced the changes in distribution due to simultaneous reactions of main-chain scission and cross-linking analytically. However, in the present case, the molecular weight distributions of the target polymers are reasonably well controlled to be less than 1.2, and the initial distributions are predicted not to play a major role in gelation. The simultaneous change in the molecular weight distribution due to radiation-induced reactions also results in a nonlinearity of eqs 1 and 2. Therefore,

Table 1. Values of $G(x)$ Determined for Various Ion Beams and Polymer Chain Lengths

	Mw ($\times 10^4$)	Mn ($\times 10^4$)	2 MeV H^+ 15 eV/nm	2 MeV He^+ 220 eV/nm	0.5 MeV C^+ 410 eV/nm	2 MeV C^+ 720 eV/nm	2 MeV N^+ 790 eV/nm
PMPS1	68−33	46−26	0.0018 (0.0021)[a]	0.0049 (0.0052)[a]	0.021 (0.022)[a]	0.072 (0.0079)[a]	0.082 (0.0095)[a]
PMPS2	20−16	15−11	0.0021	0.0095	0.052	0.081	0.15
PMPS3	3.6−3.0	2.6−2.1	0.0030	0.019	0.07	0.18	0.21
PMPS4	1.5−1.2	1.0−0.95	0.0075	0.021	0.075	0.20	0.26
PMPS5	0.71−0.60	0.52−0.45	0.019 (0.021)[a]	0.061 (0.089)[a]	0.18 (0.19)[a]	0.27 (0.33)[a]	0.34 (0.42)[a]

[a] Values in the parentheses were estimated by eqs 5 and 6.

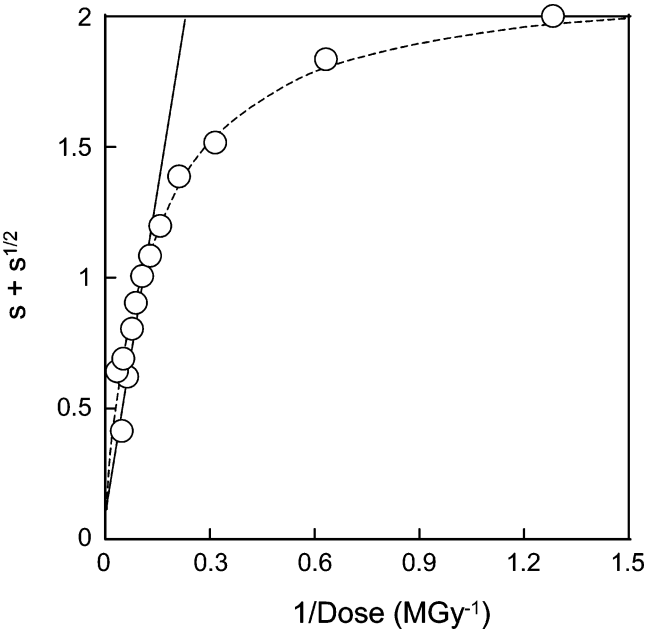

Figure 2. Charlesby−Pinner plot of $s + s^{1/2}$ vs $1/D$ for 2 MeV $^4He^+$ irradiation of PMPS1. Solid line denotes the fit by eq 1 in the high-dose region for the estimation of $G(x)$ in Table 1. Dashed line is given by eqs 5 and 6 for the entire dose region.

the following equations are proposed to extend the validity of the relationship by introducing a deductive distribution function of molecular weight on the basis of an arbitrary distribution:[14]

$$s + s^{1/2} = p/q + \frac{(2 - p/q)(D_V - D_g)}{(D_V - D)} \quad (5)$$

$$D_V = 4\left(\frac{1}{uu_n} - \frac{1}{u_w}\right)/3q \quad (6)$$

where D_g is the gelation dose, and u is the degree of polymerization. Equation 5 provides a better fit to the observed values of s at high doses than eq 1, as shown in Figure 2. However, the G values of cross-linking derived from this fit are almost identical to those in Table 1, depending on the molecular weight, because the values are estimated in the low-dose region, where eq 1 is sufficiently linear.

The effects of the polymer structure[33] and the cross-linking precursor species[34] have been considered in previous studies, where it was revealed that there was less of a dependence of cross-linking G values on the molecular weight in the case of γ-rays or electron beam irradiation. The cross-linking points in polymer materials are distributed nonhomogeneously on an ion track along an ion trajectory. A schematic of this type of nonhomogeneous distribution is shown in Figure 3. Intramolecular cross-linking, which constitutes a greater contribution to cross-linking G values in the inner region of ion tracks associated with higher densities of deposited energy, is not taken into account by the statistical treatment in eqs 1−6, and it is this case that gives rise to an underestimate of the number of cross-links. As the polymer film used in the present study is sufficiently thin to allow the change in kinetic energy of an incident particle to be neglected, a model of cylindrical energy deposition is sufficient, without needing to refer to the dependence of the radial energy distribution on the direction of the ion trajectory. The total yield of gels generated by ion-beam irradiation can thus be treated by using a simplified expression,[16,30] as follows.

$$g = 1 - \exp[-n\pi r_{cc}^2] \quad (7)$$

Here, r_{cc} is the radius of the cross-section of the cylindrical region (chemical core), and n represents the fluence of incident ions. The effect of the diffusion of reactive intermediates, determined by using a low-energy ion beam, has been formulated as the term δr[10]:

$$r_{cc} = r' + \delta r' \quad (8)$$

The value of $\delta r'$ in PMPS was determined to be 0.5−0.7 nm.[10] On the basis of traces of the gel fraction by eq 7, the estimated values of r_{cc} are summarized for 2 MeV H, 2 MeV He, 0.5−2 MeV C, 2 MeV N, and 520 MeV Kr ion beams in Table 2. The value of r_{cc} increases substantially with molecular weight in all cases except for irradiation with 2 MeV H^+, suggesting that the cylindrical scheme may not be applicable for the 2 MeV H^+ ion beam because the deposited energy density is too low to promote the cylindrical distribution of cross-links in an ion track.

AFM images of the cylindrical gel area are shown in Figure 4 for comparison with traces of the gel fraction. Equation 7 provides a good fit for the trace of the gel fraction, and the estimated values of r_{cc} for both ion beams correspond with the values observed from the AFM micrographs. Figure 5 shows a series of AFM micrographs observed for the irradiation of PMPS4 thin films with various ion beams. These images clearly reveal wormhole-like structures (nanowires) on the substrate, which is ascribed to the cylindrical formation of nanogel along ion trajectories. The value of r_{cc} depends on both the molecular weight of the target polymer and the LET of incident ions (see Table 2). Nanowires with r_{cc} of less than ~6 nm represent fragments, as observed from the nonuniform distribution of nanowire length in the micrographs for 5.1 MeV Fe or Si irradiation. As r_{cc} increases, the length of the nanowires becomes more uniform and more closely

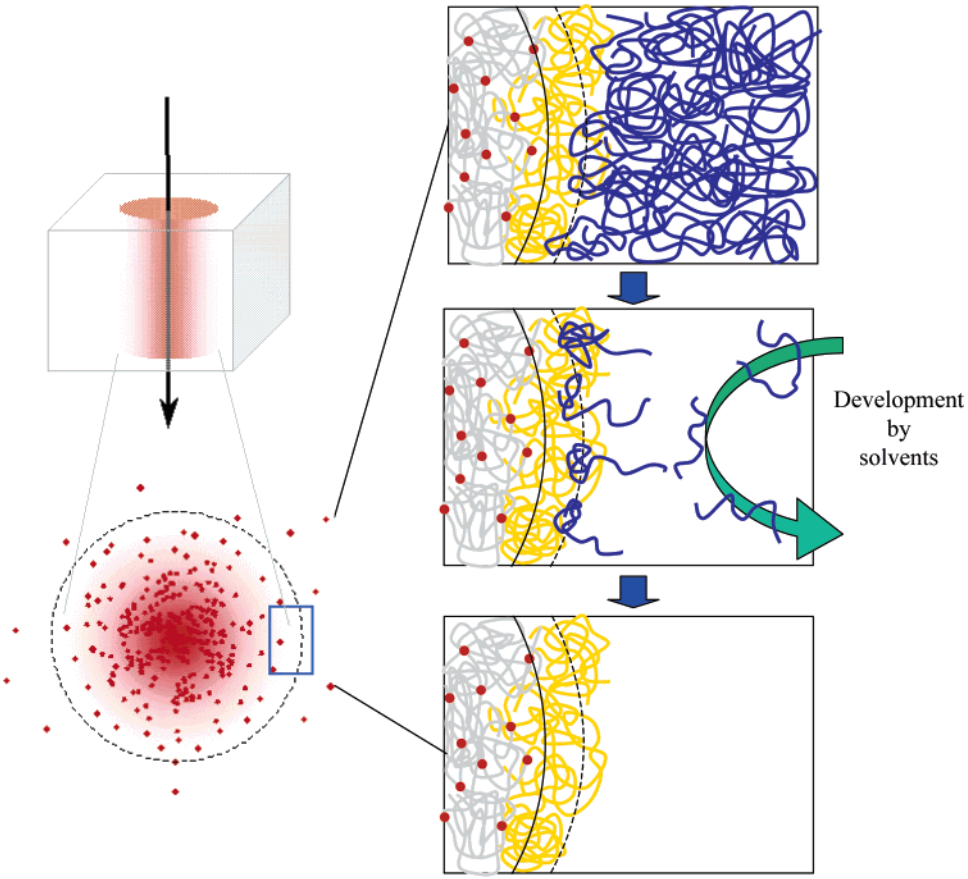

Figure 3. Schematic of the nonhomogeneous distribution of cross-links in an ion track. Dissolution of noncrosslinked molecules results in the formation of isolated nanowires.

Table 2. Values of r_{cc} for Various Ion Beams and Polymer Chain Lengths

ions	energy (MeV)	LET (eV/nm)	r_{cc} for PMPS1 (nm)	r_{cc} for PMPS2 (nm)	r_{cc} for PMPS3 (nm)	r_{cc} for PMPS4 (nm)	r_{cc} for PMPS5 (nm)
$^{1}H^{+\,a}$	2.0	15	0.15	0.15	0.14	0.14	0.15
$^{4}He^{+\,a}$	2.0	220	1.2	0.95	0.76	0.60	0.52
$^{12}C^{+\,a}$	0.50	410	2.2	2.1	1.6	1.1	0.94
$^{12}C^{+\,a}$	2.0	720	5.0	4.3	4.0	3.4	2.7
$^{14}N^{+\,a}$	2.0	790	5.1	4.8	4.2	3.8	3.0
$^{14}N^{+\,b}$	2.0	790	4.8	4.8	4.3	3.6	2.8
$^{56}Fe^{2+\,b}$	5.1	1550				5.5	
$^{28}Si^{2+\,b}$	5.1	1620				5.9	
$^{28}Si^{5+\,b}$	10.2	2150				6.1	
$^{40}Ar^{8+\,b}$	175	2200	8.2	7.3		6.1	4.0
$^{56}Fe^{4+\,b}$	8.5	2250				5.8	
$^{56}Fe^{5+\,b}$	10.2	2600				7.7	
$^{84}Kr^{20+\,a}$	520	4100	10.7	9.6	8.6	7.9	6.4
$^{84}Kr^{20+\,b}$	520	4100	10.2	9.2	8.3		6.1
$^{129}Xe^{23+\,b}$	450	8500	12.1	10.5	9.3		6.9

[a] Values estimated from gel traces by eq 7. [b] Values estimated by direct AFM observation.

matches the thickness of the target film. Thus, the winding shapes of the wires appear to be due to swelling induced by the solvent used in the development procedure. The number of nonfragmented nanowires in a unit area of substrate is consistent with the fluence of incident ions. This is also suggests that each nanowire is produced by a single ion trajectory.

Sizes of Nanowires. Our group previously reported that cross-linking reactions are mainly promoted by side-chain dissociated silyl radicals and that the predominant reaction is determined by the radical concentration in the ion tracks.[21,30,34] Thus, the distribution of cross-links in an ion track is expected to reflect the radial dose (deposited energy density) distribution, where ρ_{cr} is the critical energy density for the predominance of cross-linking in PMPS. The radial dose distribution in an ion track is thus given by[15,23]

$$\rho_c = \frac{LET}{2}[\pi r_c^{\,2}]^{-1} + \frac{LET}{2}\left[2\pi r_c^{\,2}\ln\left(\frac{e^{1/2}r_p}{r_c}\right)\right]^{-1} \qquad r \le r_c \quad (9a)$$

$$\rho_p(r) = \frac{LET}{2}\left[2\pi r^2\ln\left(\frac{e^{1/2}r_p}{r_c}\right)\right]^{-1} \qquad r_c < r \le r_p \quad (9b)$$

where ρ_c is the deposited energy density in the core area, and r_c and r_p are the radii of the core and penumbra area. For gel formation in a polymer system, it is necessary to introduce one cross-link per polymer

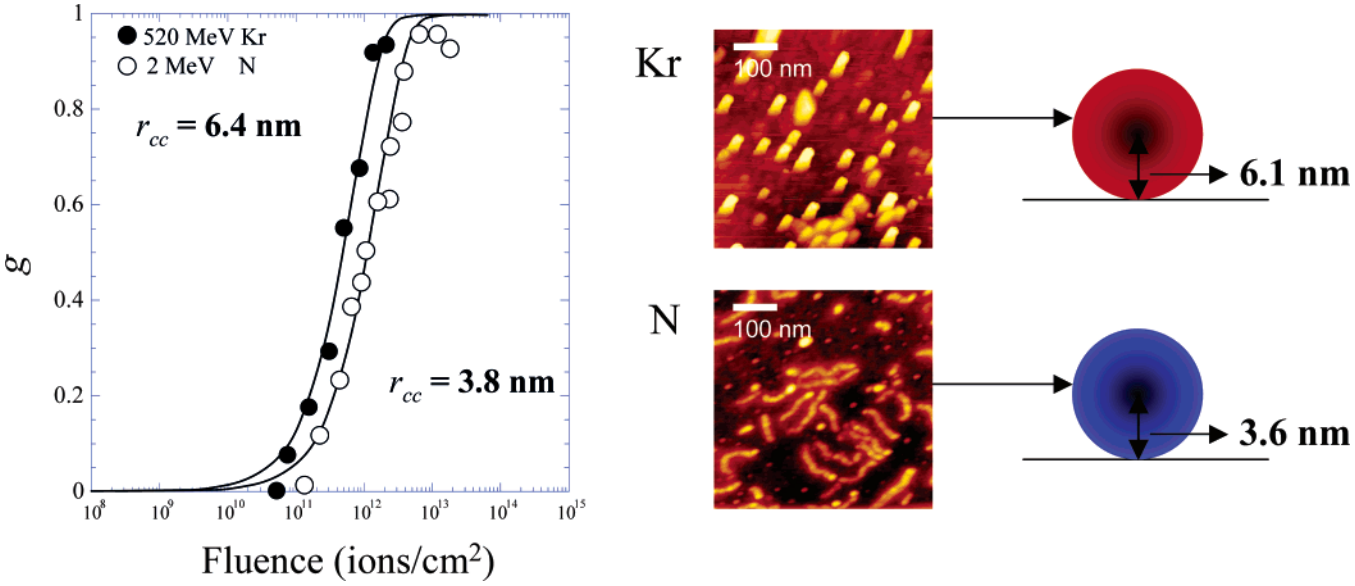

Figure 4. Gel evolution curves recorded for 520 MeV $^{84}Kr^{20+}$ irradiation of PMPS5 and 2 MeV $^{14}N^{+}$ irradiation of PMPS4. Solid lines denote the fit for the respective gel fraction based on eq 7. The estimated values of r_{cc} are 6.4 and 3.8 nm for the Kr and N ion beams. AFM micrographs were observed for the same set of polymers and ion beams. The fluence of Kr and N ions was set at 1.4×10^{10} and 6.4×10^{9} cm^{-2}, respectively.

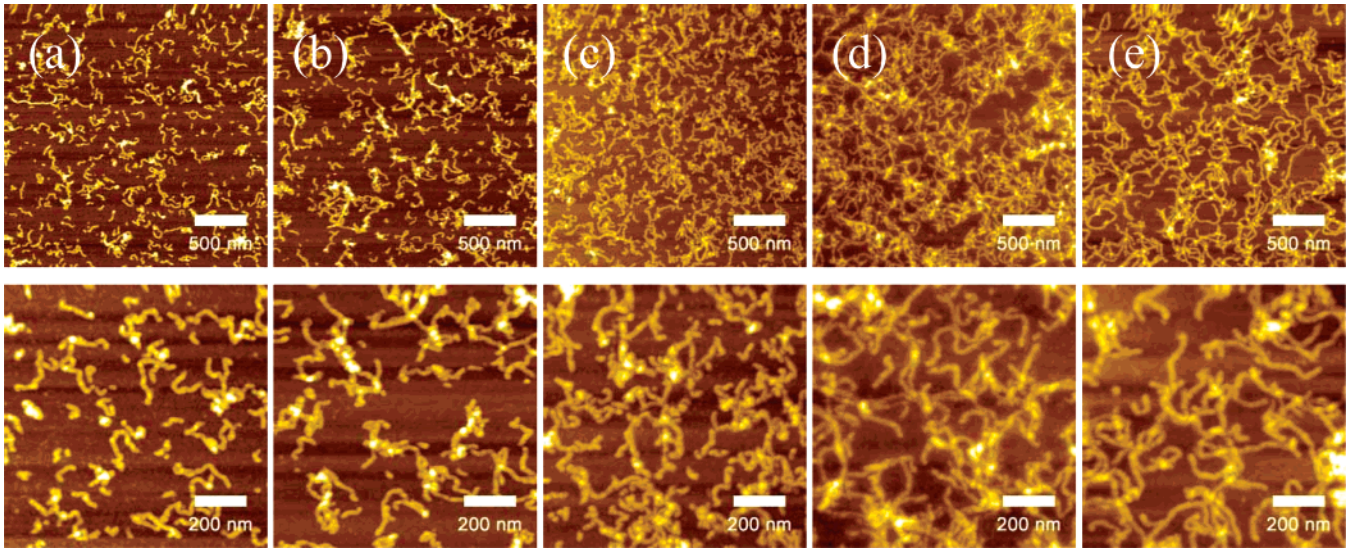

Figure 5. AFM micrographs observed after irradiation of PMPS4 with (a) 5.1 MeV $^{28}Si^{2+}$, (b) 10.2 MeV $^{28}Si^{5+}$, (c) 5.1 MeV $^{56}Fe^{4+}$, (d) 8.5 MeV $^{56}Fe^{4+}$, and (e) 10.2 MeV $^{56}Fe^{4+}$ ion beams (with fluences of (a) 5.5×10^{10}, (b) 7.9×10^{10}, (c) 8.6×10^{10}, (d–e) 5.0×10^{10} ions cm^{-2}, respectively). Micrographs in the second row are enlargements of the corresponding images above.

molecule. Assuming a sole contribution from the cross-linking reactions in the chemical core, ρ_{cr} is given by

$$\rho_{cr} = \frac{100\rho A}{G(x)mN} \tag{10}$$

where A is Avogadro's number, and N is the degree of polymerization. The value of $mN/\rho A$ reflects the volume of a polymer molecule. Substitution of $\rho_p(r)$ in eq 9b with ρ_{cr} gives the following requirement for r'.[10]

$$r'^2 = \frac{LET \cdot G(x)mN}{400\pi\rho A}\left[\ln\left(\frac{e^{1/2}r_p}{r_c}\right)\right]^{-1} \tag{11}$$

By using the reported value of $G(x) = 0.12$, derived from radiation-induced changes in molecular weight,[21] the calculated values of r_{cc} are compared with the experimental values in Figure 6. The values given by the nonempirical formulation of eq 11 are consistent with the experimental values for polymers with sufficient chain length (PMPS1 and PMPS2). However, a considerable discrepancy occurs between the calculated and experimental results for polymers with shorter chains. The global configuration of the polymer molecules depends heavily on the length of the polymer chains, leading to transformation from random coil (long chain) to rodlike (short chain) conformations. The gyration radius (R_g) of a polymer molecule, which determines the size of a molecule spreading in the media, is correlated with this transformation. The following expression was suggested for this correlation between R_g and N:

$$R_g = \kappa N^{\alpha} \tag{12}$$

where κ is a constant. The index α depends on the global configuration of the molecules, varying from 0.4 (random

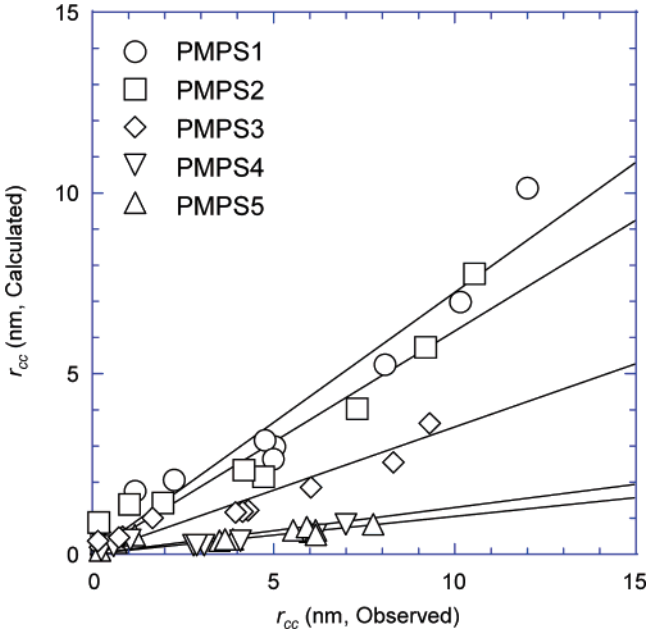

Figure 6. Correlation between r_{cc} values estimated by gel traces, direct AFM measurement, and calculations using eq 11.

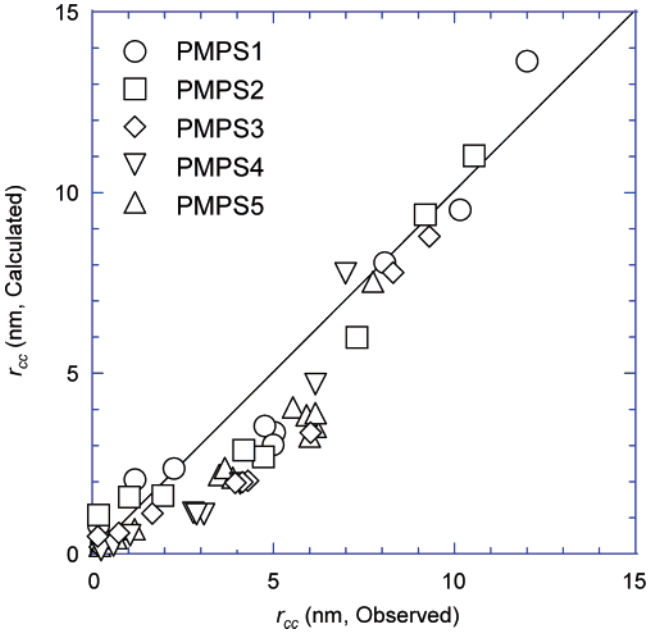

Figure 7. Correlation between r_{cc} values estimated experimentally and those calculated using eq 13.

coil) to 0.5 (rodlike). The persistence length of a chain has been reported to be 1.1 nm for PMPS,[31] and the length of a monomer repeating unit in an Si chain, derived from the Si−Si bond length of 0.2414 nm, is 0.20 nm with a dihedral angle of 114.4°.[35] On the basis of these structural parameters, the scaling law for a helical wormlike chain model[36] results in an index α of 0.410, 0.419, 0.451, 0.485, and 0.492 for PMPS1−5, respectively. Thus, the effective volume of a polymer chain can be simply calculated as $^4/_3\pi R_g^3$, and the substitution of $mN/\rho A$ in eq 10 with the effective volume leads to the expression

$$r'^2 = \frac{LET \cdot G(x) N^{3\alpha}}{400\pi\beta}\left[\ln\left(\frac{e^{1/2} r_p}{r_c}\right)\right]^{-1} \qquad (13)$$

where β is the effective density parameter of the monomer unit (kg m^{-3}). On the basis of eq 13, the calculated value of r_{cc} is plotted against the experimental values in Figure 7. All polymers, with a variety of molecular weights, follow a single trend, and the calculated values display good correspondence in the range $r_{cc} > 7$ nm. The underestimate of r_{cc} by eq 13 for $r_{cc} < 7$ nm suggests that the initial deposition of energy and the radial dose distribution estimated by eqs 9 and 10 do not account for the radial distribution of chemical intermediates and thus cannot model the concentration of cross-linking in the core of the ion track. The value of $G(x)$ increases dramatically with an increase in the density of reactive intermediates. On the basis of the assumption that $G(x)$ is a function of the density of deposited energy, the present results indicate that the yield of the chemical reaction is dependent on the energy density. Cross-linking reactions in ion tracks, therefore, have potential for not only single-particle fabrication with subnanometer-scale spatial resolution for any kind of cross-linking polymer, but also the study of nanoscale distributions of radial dose and chemical yield in an ion track.

Conclusion

On the basis of the strong dependence of the chemical yield of cross-linking reactions on the molecular weight of the target polymers, a cylindrical scheme was derived to represent the distribution of cross-links in an ion track. The total volume of the cross-linked polymer gels is well traced by the scheme. The cylindrical structures were also clearly visualized by AFM as wormlike structures (nanowires) associated with the core of ion tracks. The size of these nanowires determined by the analytical representation was confirmed to match that observed by AFM. The dependence of the size of nanowires on the chain length of the polymer and the LET of incident ions was formulated in terms of the radial variation of dose in ion tracks and the global chain configuration of the polymers, providing a good fit of the experimental results for nanowire with radius of 7 nm or greater. The present results also demonstrate the possibility of single-particle fabrication of nanostructures with subnanometer spatial resolution.

Acknowledgment. The authors thank Dr. Y. Kunimi and Dr. Y. Matsui of the Institute of Scientific and Industrial Research (ISIR), Osaka University, and Dr. T. Iwai and Mr. T. Omata of the University of Tokyo for experimental support. This work was supported in part by a Grant-in-Aid for Scientific Research from the Japan Society for the Promotion of Science (JSPS).

References and Notes

(1) Wilson, R. R. *Radiology* **1946**, *47*, 487.
(2) Fleisher, R. L.; Price, P. B.; Walker, R. M. *Nuclear Trccks in Solid*; University of California Press: Los Angeles, 1975.
(3) Spor, R. *Ion Tracks and Microtechnology*; Vieweg: Braunschweig, 1990.
(4) Fink, D. *Fundamentals of Ion-Irradiated Polymers*; Springer: Berlin 2004.
(5) Price, P. B.; Walker, R. M. *Nature*, **1962**, *196*, 732; Price, P. B.; Walker, R. M. *J. Appl. Phys.* **1962**, *33*, 3400.
(6) Fleischer, R. L.; Price, P. B. *Science* **1963**, *140*, 1221; Fleischer, R. L.; Price, P. B.; Walker, R. M. *Science* **1965**, *149*, 383.
(7) Benton, E. V. *Nucl. Instrum. Methods* **1971**, *92*, 97; Benton, E. V.; Henke, R. P. *Nucl. Instrum. Methods* **1969**, *70*, 183.

(8) Bean, C. P.; Doyle, M. V.; Entine, G. *J. Appl. Phys.* **1970**, *41*, 1454.
(9) Cartwright, B. G.; Shirk, E. K.; Price, P. B. *Nucl. Instrum. Methods* **1978**, *153*, 457; Waligorski, M. P. R.; Hamm, R. N.; Katz, R. *Nucl. Tracks Radiat. Meas.* **1986**, *11*, 309.
(10) Charlesby, A. *Proc. R. Soc. London, Ser. A* **1954**, *222*, 60; Charlesby, A. *Proc. R. Soc. London, Ser. A* **1954**, *224*, 120; Charlesby, A.; Pinner, S. H. *Proc. R. Soc. London, Ser. A* **1959**, *249*, 367.
(11) Saito, O. *J. Phys. Soc. Jpn.* **1958**, *13*, 1451; Saito, O. *J. Phys. Soc. Jpn.* **1959**, *14*, 798.
(12) Inokuti, M. *J. Chem. Phys.* **1960**, *33*, 1607; Inokuti, M. *J. Chem. Phys.* **1963**, *38*, 2999.
(13) Zhang, Y. F.; Ge, X. W.; Sun, J. Z. *Radiat. Phys. Chem.* **1990**, *35*, 163.
(14) Olejniczak, K.; Rosiak., J.; Charlesby, A. *Radiat. Phys. Chem.* **1991**, *37*, 499.
(15) Magee, J. L.; Chatterjee, A. *J. Phys. Chem.* **1980**, *84*, 3529; Chatterjee, A.; Magee, J. L. *J. Phys. Chem.* **1980**, *84*, 3537.
(16) Seki, S.; Tsukuda, S.; Maeda, K.; Matsui, Y.; Saeki, A.; Tagawa, S. *Phys. Rev. B* **2004**, *70*, 144203.
(17) Aoki, Y.; Kouchi, N.; Shibata, H.; Tagawa, S.; Tabata, Y.; Imamura, S. *Nucl. Instr. Methods Phys. Res., Sect. B* **1988**, *33*, 799.
(18) Puglisi, O.; Licciardello, A. *Nucl. Instr. Methods Phys. Res., Sect. B* **1987**, *19/20*, 865; Calcagno, L.; Foti, G. *Appl. Phys. Lett.* **1987**, *51*, 907; Licciardello, A.; Puglisi, O. *Nucl. Instr. Methods Phys. Res., Sect. B* **1988**, *32*, 131.
(19) Sasuga, T.; Kawanishi, S.; Seguchi, T.; Kohno, I. *Polymer* **1989**, *30*, 2045; Sasuga, T.; Kudoh, H.; Seguchi, T. *Polymer* **1999**, *40*, 5095.
(20) LaVerne, J. A. *J. Phys. Chem.* **1996**, *100*, 18757.
(21) Seki, S.; Shibata, H.; Ban, H.; Ishigure, K.; Tagawa, S. *Radiat. Phys. Chem.* **1996**, *48*, 539.
(22) Koizumi, H.; Taguchi, M.; Kobayashi, Y.; Ichikawa, T. *Nucl. Instr. Methods Phys. Res., Sect. B* **2001**, *179*, 530.
(23) Magee, J. L.; Chatterjee, A. *Kinetics of Nonhomogeneous Processes*; Freeman, G. R., Ed.; Wiley: New York, 1987; Chapter 4, p 171.
(24) Appleby, A. *Radiation Research*; Taylor and Francis: London, 1987; Vol. 2, p 23.
(25) LaVerne, J. A.; Schuler, R. H. *Radiation Research*; Taylor and Francis: London 1987; Vol. 2, pp 17.
(26) Burns, W. G.; Reed, C. R. V. *Trans. Faraday Soc.* **1970**, *66*, 2159.
(27) Schuler, R. H.; Barr, N. F. *J. Am. Chem. Soc.* **1956**, *78*, 5756; Schuler, R. H. *J. Phys. Chem.* **1967**, *71*, 3712.
(28) Seki, S.; Maeda, K.; Tagawa, S.; Kudoh, H.; Sugimoto, M.; Morita, Y.; Shibata, H. *Adv. Mater.* **2001**, *13*, 1663; Seki, S.; Tsukuda, S.; Yoshida, Y.; Kozawa, T.; Tagawa, S.; Sugimoto, M.; Tanaka, S. *Jpn. J. Appl. Phys.* **2003**, *42*, 4159.
(29) Tsukuda, S.; Seki, S.; Tagawa, S.; Sugimoto, M.; Idesaki, A.; Tanaka, S.; Ohshima, A. *J. Phys. Chem. B* **2004**, *108*, 3407.
(30) Seki, S.; Maeda, K.; Kunimi, Y.: Tagawa, S.; Yoshida, Y.; Kudoh, H.; Sugimoto, M.; Morita, Y.; Seguchi, T.; Iwai, T.; Shibata, H.; Asai, K.; Ishigure, K *J. Phys. Chem. B* **1999**, *103*, 3043; Seki, S.; Kanzaki, K.; Yoshida, Y.; Shibata, H.; Asai, K.; Tagawa, S.; Ishigure, K. *Jpn. J. Appl. Phys.* **1997**, *36*, 5361.
(31) Seki, S. Y.; Yoshida, Y.; Tagawa, S.; Asai, K. *Macromolecules* **1999**, *32*, 1080; Seki, S.; Koizumi, Y.; Kawaguchi, T.; Habara, H.; Tagawa, S. *J. Am. Chem. Soc.* **2004**, *126*, 3521.
(32) Ziegler, J. F.; Biersack, J. P.; Littmaek, U. *The Stopping and Range of Ions in Solids*; Pergamon Press: New York, 1985.
(33) Seki, S.; Cromack, K. R.; Trifunac, A. D.; Yoshida, Y.; Tagawa, S.; Asai, K.; Ishigure, K. *J. Phys. Chem. B* **1998**, *102*, 8367.
(34) Seki, S.; Matsui, Y.; Yoshida, Y.; Tagawa, S.; Koe, J. R.; Fujiki, M. *J. Phys. Chem. B* **2002**, *106*, 6849; Seki, S.; Tagawa, S.; Ishigure, K.; Cromack, K. R.; Trifunac. A. D. *Radiat. Phys. Chem*. **1996**, *47*, 217.
(35) Koe, J. R.; Powell, D. R.; Buffy, J. J.; Hayase, S.; West, R. *Angew. Chem., Int. Ed.* **1998**, *37*, 1441.
(36) Yamakawa, H. *Helical Wormlike Chains in Polymer Solutions*; Springer: Berlin 1997; Yamakawa, H.; Abe, F.; and Einaga, Y. *Macromolecules* **1994**, *27*, 5704.

MA051821X